Physical mechanisms affecting phytoplankton variability along the Chilean coast.

Felipe Tornquist*, Grant R. Bigg*, Robert G. Bryant*

*Department of Geography, University of Sheffield, Winter Street, Sheffield S10 2TN, UK

E-mail address: grant.bigg@sheffield.ac.uk (G.R. Bigg); Felipetornquist@hotmail.com (F. Tornquist)

keywords: sea surface temperature, chlorophyll, precipitation, coastal upwelling, background nutrients, Chile, Northern Zone, Central Zone, Southern Zone, SPSA, Ocean colour, rivers, EBUS.

Chile has high phytoplankton production due to being a classic example of an Eastern Boundary Upwelling System. Monthly averaged chlorophyll (Chl) and physical parameters (sea surface temperature, precipitation rate, southerly and westerly winds) were studied off the Chilean coast from 2002 to 2018, in order to understand the primary production along this important ocean margin. The coastal margin was split into three zones and ten sub-sections. The Northern Zone had a low phytoplankton production with small seasonal variability, except in its north. This pattern is due to a narrow shelf, weak winds, lack of precipitation and relatively stable weather conditions driven by the Southeast Pacific Subtropical Anticyclone (SPSA). The Central Zone presented a seasonally varying production, with a high Chl concentration in summer and early spring. This is linked to the SPSA movement and sunlight reduction during the winter. A high Chl activity is seen in the Southern Zone despite this Zone being at the limits of the SPSA effect, leading to weak longshore winds only during the warm season. Overall, this study has demonstrated the importance of shelf width and the upwelling driven by the presence or absence of the SPSA for ocean primary production. Thus, the most productive region is from 35°S to 45°S owing to both variables being present.

1. Introduction

Eastern Boundary Upwelling Systems (EBUS) are considered the most productive zones of the world's oceans (García-Reyes et al., 2015). They are dominated by seasonally-regulated upwelling episodes linked to alongshore winds (Mogollón and Calil, 2017; Vergara et al., 2017). These winds force the surface waters offshore to be replaced with nutrient-rich deep water. This phenomenon is known as the Zonal Ekman Transport (ZET; Yuras et al., 2005; Corredor-Acosta et al., 2015; Echevin et al., 2014; Gómez et al., 2012). There are many EBUSs, such as off California, Morocco, and Namibia, but the most productive is in the Peru-Chilean region, owing to the Southeast Pacific Subtropical Anticyclone (SPSA) and Humboldt Current System (HCS). The SPSA creates favourable winds for upwelling, while HCS causes the water to be even colder and transports the nutrients northwards (Ancapichun and Garcés, 2015; Yuras et al., 2005; Gómez et al., 2017). As a result, the annual cycles of phytoplankton and primary production are significant, making the Peru-Chile coast responsible for more than ten percent of the worldwide marine fisheries (Vergara et al., 2017; Mongollón and Calil, 2017; Corredor-Acosta et al., 2015; Gómez et al., 2012; Yuras et al., 2005).

In the particular case of Chile, the phytoplankton concentrations display significant spatial variation due to the long latitudinal coastal extension, over which the atmospheric temperatures slowly decrease and the rainfall increases southwards (CONAMA, 2008). These are themselves driven mainly by the SPSA and the HCS, which are intermittently perturbed by the Pacific Decadal Oscillation (PDO), EL Niño Southern Oscillation (ENSO), and Antarctic Oscillation (AAO; Mogollón and Calil, 2017; Ancapichun and Garcés, 2015). The SPSA generates a high-pressure system around the coast that compresses and heats the descending air mass, creating stable atmospheric conditions (Schultz et al., 2012). Another factor is the Andes, whose high elevations of over 5,000 m contain snowpacks in their peaks, which provide a primary freshwater source for fluvial systems draining to the coast (Cordero et al., 2019). Additionally, the Andes constrain the meridional spread of the SPSA, enhancing its effectiveness and leading to dry weather in Chile and wet conditions in the Amazon basin (Barrett et al., 2009; Schultz et al., 2012; Garreaud, 2009).

The Chilean coast is generally grouped into three Zones with very distinctive properties: the Northern (18°-30°S), Central (30°-40°S) and Southern Zones (40°-56°S; Thiel et al., 2007; CONAMA, 2008; Figure 1). The Northern Zone has a climate that is extremely arid, with almost no precipitation (Schultz et al., 2012). The Central Zone exhibits a Mediterranean-like climate, where most of the precipitation occurs during a few winter storms (Garreaud et al., 2020). Finally, the Southern Zone is considered to have a hyper-humid climate (Aguayo et al., 2021). The cycles mentioned in the northern and Central Zones are driven by SPSA movement to the north during the winter, allowing more stable weather conditions in the north and precipitation events during the winter (Aguirre et al., 2021). By contrast, the Southern Zone is only affected by the SPSA in the summer south to around 42°S (Ancapichun and Garcés, 2015).

The Northern and Central Zone coastlines are relatively straight (N-S; Figure 1). However, the coastal topography produces current variations that are hard to predict (Thiel et al., 2007). This leads to the formation of complex bay circulation systems, with counter-rotating gyres, which could affect the plankton dynamics. This is more marked in the Southern Zone due to its intricate geography; with many archipelagos and fjords mainly located south of Chiloe Island (Iriarte et al., 2007). At the same time, along the Chilean coast there exist areas with strong upwelling due to their topographic capes generating eddies and filaments. These are in Mejillones-Antofagasta (23.1°-23.6°S), Coquimbo (30°S), Valparaiso (33°S) and Concepción (36.8°S; Figure 1; Thiel et al., 2007; Gómez et al., 2012).

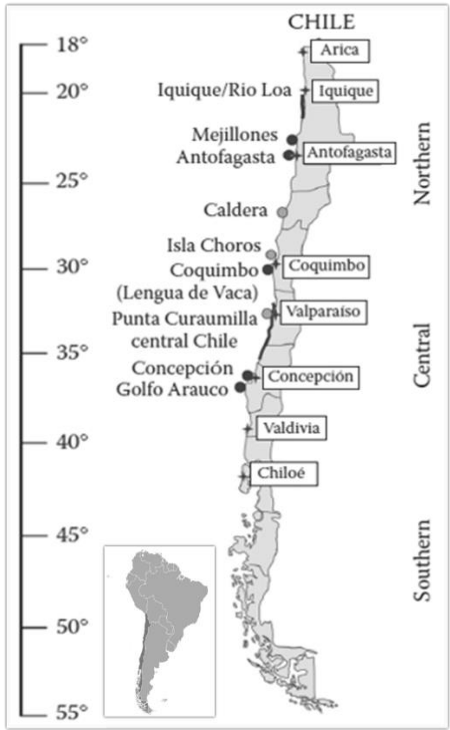

Figure 1. Study area with the principal upwelling regions located, the grey points are Zone with frequent upwelling, while the black dots are the main upwelling filaments zones. Finally, the black lines show the coastal sections with occasional upwelling (Thiel et al., 2007).

Another significant difference between Zones is the ocean shelf width, which is a key factor in the ocean remineralisation process (Thiel et al., 2007). The Northern Zone has a narrow continental shelf, in places of less than 10 km width (Ancapichun and Garcés, 2015; Marchant et al., 2007; Jacob et al., 2011). However, the region near Peru has a broad shelf that continues north until Arica (Echevin et al., 2014; Thiel et al., 2007; Cortés et al., 2017). This shelf below 10 km width continues south until 35°S (Marchant et al., 2007). Then, its width southwards until 40°S varies from 40 to 70 km, except near the Arauco Peninsula (37-38°S), where it reduces to 12 km (Thiel et al., 2007; Marchant et al., 2007). Finally, the Southern Zone along with its intricate geography, has a shelf over 70 km wide and reaching more than 100 km at 46°S (Strub et al., 2019; Marchant et al., 2007). The shelf edge has a depth of 150-200 m (Marchant et al., 2007; Cortés et al., 2017).

Previous studies have mainly covered specific zones of Chile; specifically, the Central-Southern Zone (e.g. Vergara et al., 2017; Corredor-Acosta et al., 2015; Gómez et al., 2017; Ferreira et al., 2020). This leaves much of the long and varied Chilean coast unstudied. This is very important because the Chilean coastline has an evident multi-zone character, from experiencing the southern end of the Peruvian high productivity through a region with less production and less extensive production to a higher production region in the Southern Zone. Therefore, this overall study covers the whole territory and will help to understand which regions are more productive. This information is also valuable as a first stage for developing better fisheries strategies.

This study aims to understand and quantify the physical mechanism that controls alongshore phytoplankton production along the entire Chilean coastline [18.3°S to 53.5°S]. The objectives are (i) to estimate the trends in seasonal, interannual and spatial variability for parameters that are known to affect phytoplankton production and (ii) to compute an order of magnitude analysis of the main nutrient sources.

2. Material and Methods

2.1. Study Area

Each hydroclimatic zone along the Chilean coast was studied [North[N], Central[C] and South[S]], and these were further subdivided into 3 or 4 subsections [N1, N2, etc] (Figure 2). The main criterion used in generating these zones were (i) to account for the complexity of the coastline, and likely variation in phytoplankton behaviour in relation to significant capes and embayments, and (ii) maintaining a 100-150 km sample width across the coastal edge. The relative simplicity and roughly straight N-S-oriented coastline (Thiel et al., 2007), particularly in the Northern Zone facilitated sub-division into three subsections (Figure 2). On the other hand, the Central Zone geography has a more pronounced curved area, especially in the region 32.7-35°S so here, four subsections were used. Additionally, we note that subsections 3C and 4C have been intensively studied previously due to their relatively high recorded phytoplankton production (e.g. Vergara et al., 2017; Corredor-Acosta et al.,2015). Thus, some of our subdivisions were designed to allow direct comparison with past work. The Southern subsection includes a more complex domain (Lara et al., 2010). Here the sub-sections were selected to focus on Chiloé Island [subsection 1S], one of the most studied territories (Figure 2). The 2S-3S subsections were chosen to account for an increasing curve in the coastal edge between 45.8°-47°S. Although the area from 47°-50°S is relatively straight, westerly winds start to dominate from 50° to 53.5°S, and thus we adjust the final subsection (3S; 50°-53.5°S) to have a width of 250 km.

Within the study area, the Chilean coastal shelf width is variable and locally defines the nearshore and offshore subsection delimitation used here (Thiel et al., 2007). Authors like Vergara et al. (2017), Yuras et al. (2005), and Gómez et al. (2017) considered a 100 km offshore distance to define their study area. However, this value is approximately the maximum Chilean shelf width located in the Southern Zone (Thiel et al., 2007). Both nearshore and offshore subsections, are expected to exhibit different phytoplankton concentrations due to the likely change in depth and other mechanisms (i.e., upwelling) noted above. However, a paired study of each is important because their behaviour might be related over time. For that reason, the coastal strip region studied here was widened to move beyond the coastal shelf and coded as T [Terrestrial], and O [Oceanic]. We include a distance where the surface waters are dragged during the upwelling in Chile's Northern and Central Zones (Thiel et al., 2007). Therefore, the width per subsection was defined as between 1°-1.5°, equivalent to almost 100-150 km. This ensures that the whole shelf is part of each nearshore subsection and is consistent with the width used by the mentioned authors. Typical ocean depths at the edge of the offshore and nearshore subsection vary between 2,600-5,000 m, except for 1NT, which has a maximum depth of 778 m in its edge subsection. This is the shallowest of the sample scheme. This border is at the limit of Peru and presents a curve that increases the shelf width in that area. As such, 1NT is a relatively small subsection that is only impacted by this change in shelf width at its northern termination.

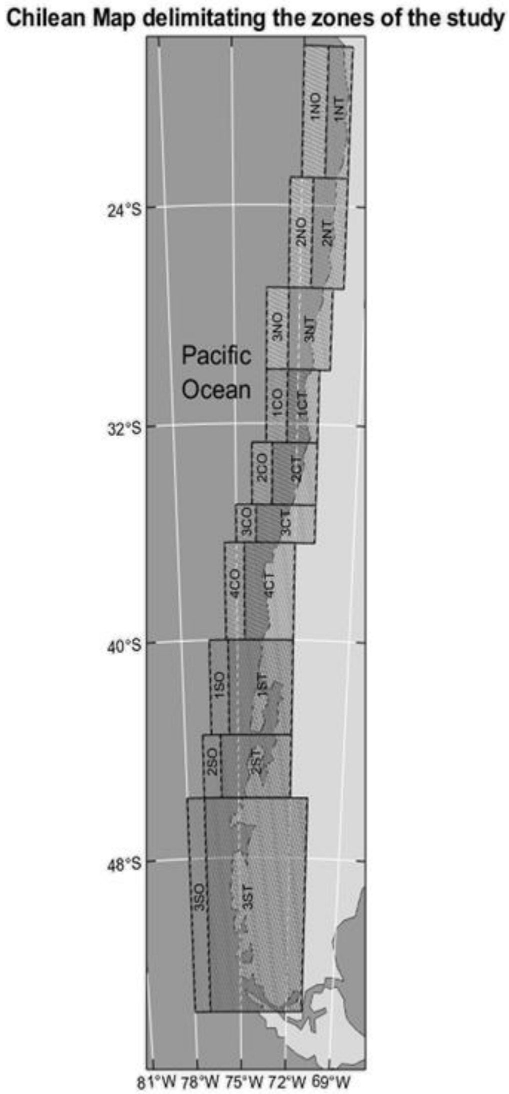

FIGURE 2. CHILEAN MAP DELIMITING THE ZONES (N: NORTH, C: CENTRAL AND S: SOUTH) OF STUDY AND ITS SUBSECTION (T: TERRESTRIAL, O:OCEANIC).

2.2. Variables Selection and Data Collection

The main variable, Chlorophyll-α (Chl) is a proxy for phytoplankton biomass, which acts as a proxy for phytoplankton concentration, and which it can be routinely obtained via remote sensing e.g. MODIS-Aqua (Franz et al., 2005; Falkowski, 1994). Although Chl measured by MODIS-Aqua [Ocean Color 3M algorithm; https://oceancolor.gsfc.nasa.gov/] gives an adequate estimate of phytoplankton concentration, it is known that algorithm retrieves in the shallow coastal region, where phytoplankton is usually present, due to the combined impacts of bottom reflectance and turbidity (Yang et al., 2018; Abbas et al., 2019). However, this relative lack of precision is minimised here as we focus upon monthly Chl tendencies across a relatively long time series [2002-2018].

The primary physical mechanism affecting phytoplankton within the study region is upwelling along the Chilean coast. This phenomenon is provoked by equatorward coastal winds (Mogollón and Calil, 2017; Vergara et al., 2017). Upwelling also brings deep cold and nutrient rich water to the surface. So, it creates a temperature decrease in the surface and sub-surface (Ancapichun and Garcés, 2015; Yuras et al.,2005). Thus, SST, wind speed, and direction are vital factors in the investigation, because these wind components make it possible to estimate upwelling and therefore the relative nutrient addition to the surface.

The precipitation rate (PR) was included as well. The PR parameter tends to exhibit contrasting trends in the Northern and Southern Zones, while the Central Zone presents an intermediate behaviour (Thiel et al., 2007). This parameter is likely to affect phytoplankton differently, depending on the amount of rain and the season of occurrence. For example, Thompson et al. (2015) found a positive relationship with the Chl when rainfall occurs during the warm season (spring-summer). Nonetheless, PR does not have the same effect during the cold seasons (autumn-winter). The data were mainly collected from satellite imagery and reanalysis methods extracted by the website GES DISC (Goddard Earth Sciences Data and Information Services Centre) Interactive Online Visualization and Analysis Infrastructure (GIOVANNI; https://giovanni.gsfc.nasa.gov/giovanni/) summarised in Table 1.

TABLE 1. PARAMETERS USED FROM THE GIOVANNI DATABASE (NASA, 2018).

Parameter	Unit	Source	Temp res.	Spatial res.
Chl	mg m^{-3}	MODIS-Aqua	Monthly	0.04° x 0.04°
SST 11µm (day)	°C	MODIS-Aqua	Monthly	0.04° x 0.04°
Precipitation Rate	mm mth^{-1}	TRMM	Monthly	0.25°x 0.25°
Westerly wind (10m)	m s^{-1}	MERRA-2	Monthly	0.63° x 1.25°
Southerly wind (10m)	m s^{-1}	MERRA-2	Monthly	0.63° x 1.25°

The period studied here was from July 2002 to June 2018. This period was chosen because it aligns with the availability of a continuous time series of MODIS-Aqua Chl data. In this way it was possible to avoid uncertainty arising from the use of different sensor and orbital parameters (Franz et al., 2005). For the first objective, these values were averaged on a monthly basis per Zone and subsection. These data were initially interrogated using boxplots and summary statistical analyses, both seasonally and interannually. Following this, relationships between Chl and other parameters were studied using correlation analysis per subsection. Here, Spearman correlation was selected instead of Pearson as the variable response in each subsection was typically skewed, thereby not confirming with assumptions associated with normal distribution (Xiao et al., 2016).

The ZET calculation (see below for details) was also done using these data, but it was averaged per Zone and season. Background nutrient concentrations of NO_3^-, SiO_4^{2-} and PO_4^{2-} were obtained from García et al. (2010) in the World Ocean Atlas (2009). Finally, it was compared the nutrient addition by upwelling, precipitation and main rivers addition.

The upwelling nutrient was estimated using the equations below. The rivers addition in the Central Zone was previously estimated by Masotti et al. (2018), meanwhile the Southern Zone rivers were computed based on averaged fluxes multiplied by the typical nutrient concentrations reported by Castro (2010).

Even though no studies about the nutrient concentration in the rainfall in the South Pacific were found in this investigation, they can be inferred from South Atlantic data. Baker et al. (2010), which are approximately 2.8-3.5 nmol m^{-3} and 0.0124-0.0146 nmol m^{-3} for NO_3^- and PO_4^{2-}, depending on the PR intensity. The SiO_4^{2-} is negligible in the PR, so only NO_3^- and PO_4^{2-} were considered.

2.3. Upwelling calculation

ZET can be calculated to estimate the upwelling and define how much nutrient is supplied to the surface. ZET depends on the meridional wind stress (WS_y). Although this variable is not obtained by satellite imaging, it can be derived from wind speed using the following equation (Gómez et al., 2012).

$$WS_y = \rho_a \cdot C_d \cdot (V) \cdot VW \quad (1)$$

Where ρ_a is air density (1.2 kg m^{-3}), C_d is the drag coefficient (0.0012) based on observational data for winds below 10 m s^{-1}, (V) is the wind speed, and VW is the southerly wind component. Then, the ZET is calculated (Ancapichun and Garcés, 2015; Gómez et al., 2012; Liao et al., 2016). Here, the geostrophic transport is considered negligible (Liao et al., 2016).

$$ZET = \frac{WS_y}{\rho_w f} \quad (2)$$

Where ρ_w is the seawater density (1026.97 kg m^{-3}), and f is the Coriolis effect. The Coriolis effect can be easily estimated by $2\Omega sin\theta$; where Ω is the Earth's angular velocity (7.292·10^{-5} s^{-1}) and θ is the latitude of the study area. Negative ZET values imply offshore transport or the opposite if it is positive (Ancapichun and Garcés, 2015; Gómez et al., 2012). The vertical speed of the ZET determines the speed of upwelling or downwelling, here called the Ekman pumping (EP), and is defined by the following equations (Ancapichun and Garcés, 2015; Ancapichun, 2012; Bravo et al., 2016).

$$EP = \frac{Curl(WS)}{\rho_w f} + \frac{\beta \cdot WS_x}{\rho_w f^2} \quad (3)$$

$$Curl(WS) = \frac{WS_y}{\partial x} + \frac{WS_x}{\partial y} \quad (4)$$

The second term of Eq.3 is generally rejected because β represents the rate of variation of the Coriolis between the latitudes in the Ekman transport, which is insignificant (Bravo et al., 2016). The Curl represents the Ekman's spiral spin (Bigg, 2003). Finally, the upwelling nutrient concentration (mmol m^{-1} s^{-1}) can be obtained as total vertical transport multiplied by the concentration of that nutrient at the depth of the Ekman layer (Liao et al., 2016).

$$N_{supply} = ZET \cdot (N_D)_{Rossby} + EP \cdot (N_D)_{coastal\ band} \quad (5)$$

The depth of the Ekman layer can be estimated in many ways. Vergara et al. (2017) suggest an 80-100m depth in the Central Zone. The concentration multiplied by the ZET is at the coast but with a Rossby radius deformation product of the Coriolis variation along the latitude. Therefore, the radius will be shorter at higher latitudes. In comparison, the EP is multiplied by the concentration at depth D but on the coast edge defined by the shelf width (Liao et al., 2016).

3. Results

The overall PR tended to increase poleward, as expected from large-scale climate considerations (Table 2). Therefore, in general, the further south the subsection was located, the more rainfall there was. The ocean strip PR (not shown) showed similar values to the coastal strip, but the latter was slightly lower, except for 3S, where its ocean strip had higher PR. SST was the only parameter that presented a similar seasonal behaviour across the whole system, with a poleward decrease of 0.5°-1.5°C per subsection (Table 2), except for subsections 2S to 3S, where there was a difference of -2°C. The highest value was reached in February (January in 1N) and the lowest value in August. The seasonal SST variability was very low, except for the warmest months. These high variations during the summer were more evident at the coast. In general, SST was driven by the annual cycle in the whole climate system with minor variations.

Table 2. Statistical summary of PR (mm month^{-1}) and SST (°C) per subsection in the coastal strip, where μ is the mean and SD is the Standard Deviation.

Zones	Northern Zone			Central Zone				Southern Zone		
Subsection	**PR1NT**	**PR2NT**	**PR3NT**	**PR1CT**	**PR2CT**	**PR3CT**	**PR4CT**	**PR1ST**	**PR2ST**	**PR3ST**
Max	15.00	20.52	79.55	108.96	170.94	275.04	289.52	276.03	277.60	164.00
μ	2.43	2.90	3.58	11.38	33.02	56.43	87.49	108.57	124.46	84.40
SD	2.70	3.71	8.00	18.14	42.56	62.09	69.79	59.19	48.41	26.42
Min	0.02	0.01	0.00	0.03	0.05	0.06	2.34	22.38	35.66	35.75
Higher than (μ+2SD)	9	11	7	11	11	10	9	10	6	6
Lower than(μ-2SD)	0	0	0	0	0	0	0	0	0	0
Subsection	**SST1NT**	**SST2NT**	**SST3NT**	**SST1CT**	**SST2CT**	**SST3CT**	**SST4CT**	**SST1ST**	**SST2ST**	**SST3ST**
Max	24.51	23.01	21.94	21.24	20.51	18.84	17.34	16.81	15.48	13.07
μ	19.99	18.40	16.82	15.90	15.44	14.50	13.98	12.93	11.78	9.72
SD	2.00	2.32	2.20	2.04	1.92	1.62	1.71	1.82	1.79	1.53
Min	15.62	13.90	13.01	12.32	11.98	11.42	10.66	9.89	8.89	6.74
Higher than (μ+2SD)	1	0	4	4	5	4	0	2	1	5
Lower than(μ-2SD)	2	0	0	0	0	0	0	0	0	0

Table 3. Statistical summary of southerly and westerly winds VW and UW in (m s^{-1}) per subsection in the coastal strip.

Zones	Northern Zone			Central Zone				Southern Zone		
Subsection	**VW1NT**	**VW2NT**	**VW3NT**	**VW1CT**	**VW2CT**	**VW3CT**	**VW4CT**	**VW1ST**	**VW2ST**	**VW3ST**
Max	4.88	7.70	10.35	10.78	10.08	11.37	9.41	5.60	5.32	3.83
μ	3.93	5.06	6.51	7.02	5.45	5.27	3.25	0.58	-0.21	-1.79
SD	0.35	0.88	1.36	1.70	2.13	2.83	3.10	2.25	2.09	1.99
Min	2.68	3.01	3.09	2.79	-0.34	-2.69	-4.25	-4.28	-4.89	-7.21
Higher than (μ+2SD)	4	8	5	2	2	1	0	3	8	8
Lower than(μ-2SD)	3	1	3	5	6	7	5	2	2	4
Subsection	**UW1NT**	**UW2NT**	**UW3NT**	**UW1CT**	**UW2CT**	**UW3CT**	**UW4CT**	**UW1ST**	**UW2ST**	**UW3ST**
Max	2.14	2.20	2.99	2.40	3.96	4.30	3.84	5.37	6.94	8.72
μ	1.59	1.75	1.98	1.61	2.38	2.56	1.99	2.48	3.73	5.18
SD	0.31	0.19	0.32	0.42	0.80	0.90	0.92	1.14	1.56	1.92
Min	0.86	1.29	1.25	0.59	0.56	0.25	-1.41	-3.06	-4.03	-3.08
Higher than (μ+2SD)	0	6	3	0	0	0	1	1	2	0
Lower than(μ-2SD)	3	4	4	2	5	3	6	5	6	3

VW presented a southerly wind dominance with a seasonal behaviour such that this variable's values reached a maximum in summer and decreased during winter from 1C to 2S (Table 3). This seasonality increased polewards with 4C reaching the higher range. The Southern Zone exhibited the opposite effect decreasing the seasonal difference further south (Table 3). 4C and 1S had northerly winds during the winter. The 3S general trend was to have northerly winds the entire year, whereas 2S's southerly winds were more frequent in the summer, particularly in February. The UW (Westerly Wind component) showed westerly wind dominance with weak values and a low variation in 1N-1C, while this component was more significant in 2S-3S (Table 3). The rest of the subsections had intermediate UW values. The behaviour of this component showed weak values during the winter and strong during the summer over 2C and 3C. From 4C to 3S, UW's seasonal trend was not influenced by the seasons, but it had a significant variation. This was more marked in 2S and 3S, where westerly winds reached magnitudes over 7 m s^{-1} in the winter and 5 m s^{-1} in the rest of the year.

Figure 3 and Table 4 indicate that in terms of Zones, the Southern Zone had the highest productivity, followed by the Central Zone. Although the Northern Zone usually had the lowest Chl coastal levels, the subsection close to Peru (1NT) had slightly higher productivity. In terms of subsections, 2NT to 1CT showed the lowest Chl concentration but with very similar variability. However, 1CT had more outliers than the rest, reaching the highest concentrations among this group.

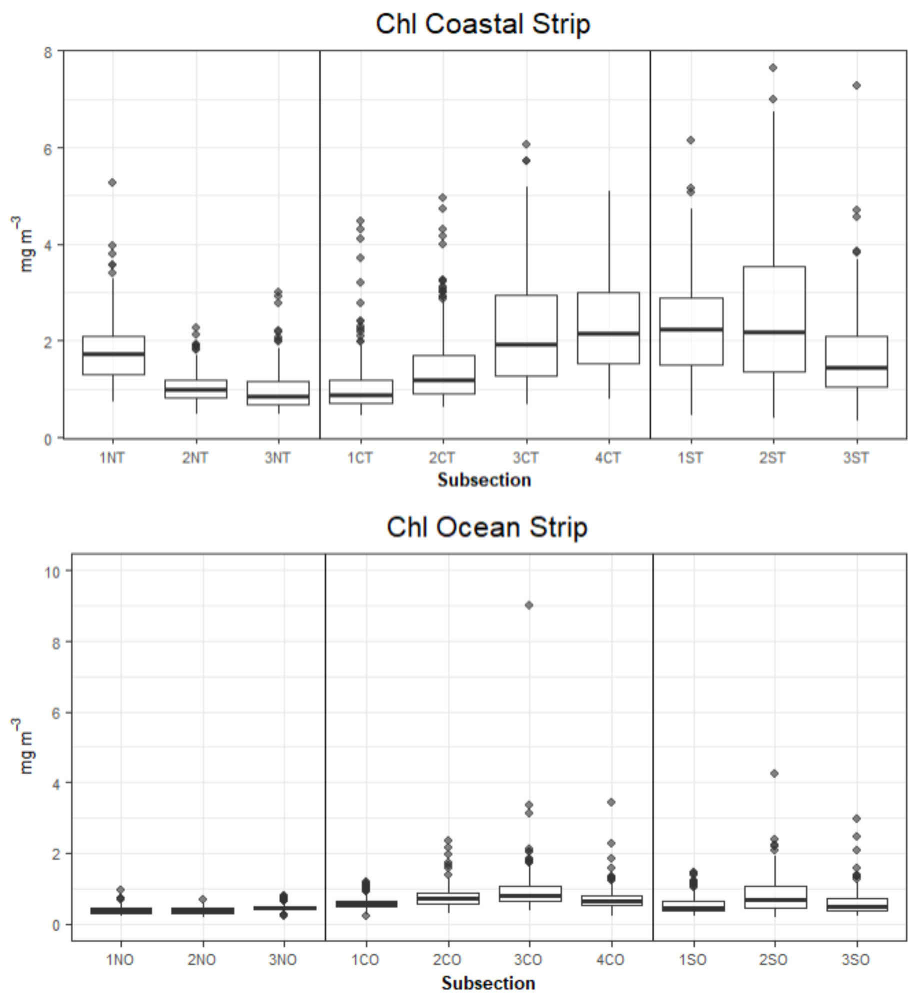

FIGURE 3. CHL BOXPLOT FOR EACH SUBSECTION, SEPARATED BY ZONE AND STRIP. SEE FIGURE 2 FOR ZONE DEFINITION.

The higher productivity was reached in 3CT to 2ST, followed by 3S and 1NT, while the lower production was in 3NT and 1CT. This was unexpected because the SPSA, responsible for longshore winds, is more intense in 3NT and 1CT while it generally is not present in the Southern Zone (Table 3; Aguirre et al., 2021; Ancapichun and Garcés, 2015).

The ocean strip had lower Chl levels than the coast, with low variability in the complete system (Figure 3). From 1NO to 1CO, the variability was particularly low, while the rest exhibited a slightly higher variability. Effectively, from 3CO towards 3SO, the number of extreme outliers increased significantly.

Table 4. Statistical summary of the Chl (mg m^{-3}) per subsection in the coastal and ocean strip, where µ is the mean and SD is the Standard Deviation.

Zones	Northern Zone			Central Zone				Southern Zone		
Subsection	**Chl1NT**	**Chl2NT**	**Chl3NT**	**Chl1CT**	**Chl2CT**	**Chl3CT**	**Chl4CT**	**Chl1ST**	**Chl2ST**	**Chl3ST**
Max	5.25	2.25	2.99	4.47	4.94	6.06	5.08	6.15	7.64	7.27
µ	1.80	1.04	0.99	1.08	1.45	2.21	2.36	2.28	2.55	1.66
SD	0.68	0.32	0.45	0.64	0.80	1.17	1.04	1.03	1.46	0.90
Min	0.75	0.48	0.50	0.46	0.61	0.68	0.78	0.46	0.39	0.34
Higher than (µ+2SD)	9	10	8	8	10	9	9	7	7	7
Lower than(µ-2SD)	0	0	0	0	0	0	0	0	0	0
Subsection	**Chl1NO**	**Chl2NO**	**Chl3NO**	**Chl1CO**	**Chl2CO**	**Chl3CO**	**Chl4CO**	**Chl1SO**	**Chl2SO**	**Chl3SO**
Max	0.96	0.67	0.81	1.17	2.34	9.01	3.44	1.45	4.23	2.96
µ	0.39	0.38	0.46	0.59	0.77	0.96	0.70	0.54	0.81	0.59
SD	0.12	0.09	0.10	0.17	0.31	0.72	0.34	0.24	0.50	0.35
Min	0.21	0.18	0.21	0.23	0.31	0.36	0.20	0.23	0.17	0.21
Higher than (µ+2SD)	7	4	8	10	6	3	4	10	8	7
Lower than(µ-2SD)	0	3	2	2	0	0	0	0	0	0

These results showed that the three Zones have different Chl concentrations. These connections were also studied by Spearman correlations in Table 5. This shows that the Northern Zone has almost no relationship between the Chl and the other parameters except for Chl~VW in 3NT. In the Central Zone Chl~VW were statistically significant in the whole Zone, excluding 2CT. These were more statistically significant in 3CT-4CT. Effectively in these subsections all the physical parameters were statistically significantly linked to Chl, but with negative correlations. On the other hand, the Chl in the Southern Zone showed significant correlations with both wind components, especially in 1ST. The Chl~PR in this Zone had a significant negative relationship, especially in 1ST, while 2ST and 3ST were slightly lower. Whereas the SST was only statistically significant in 3ST.

Table 5. Chl regression with the physical parameters per subsection in the coastal strip, the statistically significant correlations are underlined (0.01<P-values<0.05), and the statistically very significant are in bold (P-values<0.01).

Rho	Chl~SST	Chl~PR	Chl~VW	Chl~UW
1NT	-0.10	0.14	0.07	-0.12
2NT	-0.13	0.05	0.09	-0.03
3NT	-0.12	-0.08	**0.21**	0.10
1CT	*-0.16*	-0.07	**0.20**	-0.03
2CT	-0.15	0.04	0.08	0.06
3CT	**-0.19**	**-0.20**	**0.27**	**0.20**
4CT	**-0.20**	**-0.33**	**0.38**	**-0.27**
1ST	-0.06	**-0.39**	**0.45**	**-0.41**
2ST	0.15	**-0.24**	**0.26**	**-0.29**
3ST	**0.20**	**-0.20**	**0.23**	**-0.32**

4. Discussion

As it was mentioned in section 2.2 it is known that the algorithm retrieves in the shallow coastal zone, where phytoplankton is usually present. However, this relative lack of precision is not as relevant because here we are discussing monthly Chl tendencies across a relatively long time series [2002-2018] in long extension.

The different possible sources of nutrients are discussed in section 4.1, including rough estimations of the nutrient addition by upwelling, precipitation and main rivers per subsection. With this information it is possible to estimate which of these sources is more significant. Finally, the results and the nutrient analysis will be discussed per Zone in section 4.2.

4.1. Nutrient Quantification Analysis

In this section, the background average nutrients distribution is discussed. Then, nutrients brought by the upwelling (section 4.1.2), precipitation (section 4.2.3) and the main rivers (section 4.2.4) per subsection are estimated. After that, these nutrients will be compared with WS and the PR to determine a possible relationship.

4.1.1. Background Nutrients

The background nutrient concentrations data were obtained from García et al. (2010) in the World Atlas Ocean (2009). This data was used to create Figures 4 and 5 that show the surface and 100 m depth concentrations of NO_3^-, PO_4^{-2} and SiO_4^{-2} per season. The nutrients at 100 m deep are required to estimate the flux that is brought by the upwelling. This depth is based on Vergara et al. (2017) who reported that 80-100 m is the typical depth of the upwelled water in the Central Zone. The nutrients at the surface will be compared with the PR and WS.

The first observation about these nutrients is that they are very high in the extreme Southern Zone (3ST) on the surface, with a higher concentration of NO_3^- and PO_4^{2-}, while SiO_4^{2-} was only in spring (Oct-Dec). Also, the Peruvian Zone has a higher nutrient concentration than other regions except for 3ST. Additionally, NO_3^- showed higher levels at the surface in the Central Zone in the summer (Jan-Mar) and a bit lower in 1NT and 1CT to 3CT during the autumn (Apr-Jun). These subsections also exhibited a high PO_4^{2-} concentration from January to September. For the 100 m depth, NO_3^- was intense from 3NT to 4CT during the warm season. The other two seasons, 1NT, 2CT and 3CT, exhibited higher concentrations. These subsections also exhibited a high PO_4^{2-} concentration during summer, autumn and spring. Winter only showed a high concentration in 1NT.

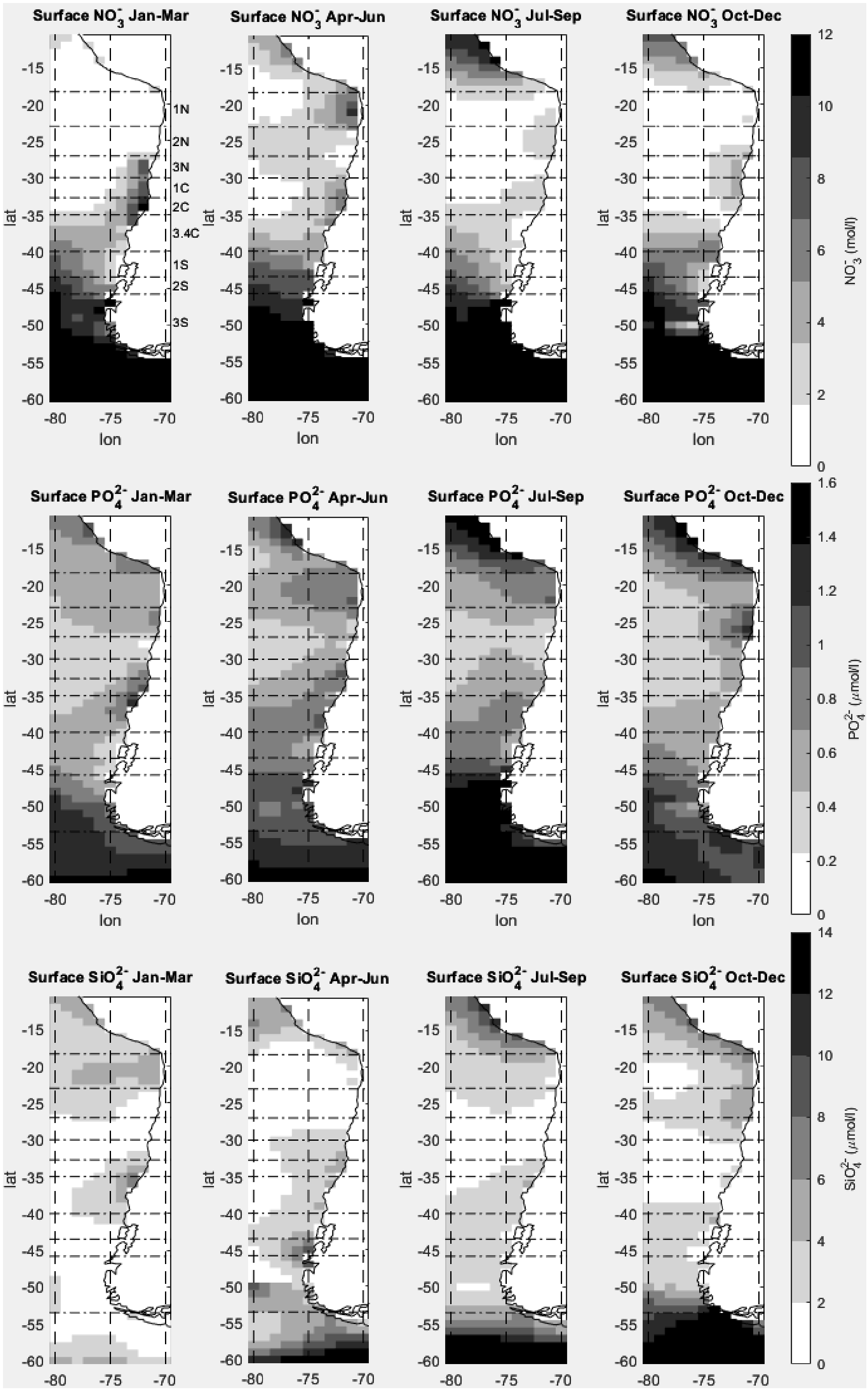

Figure 4. NO_3^- (mol·L^{-1}), PO_4^{2-} (µmol·L^{-1}), and SiO_4^{2-} (µmol·L^{-1}) surface seasonal concentrations data from García et al. (2010).

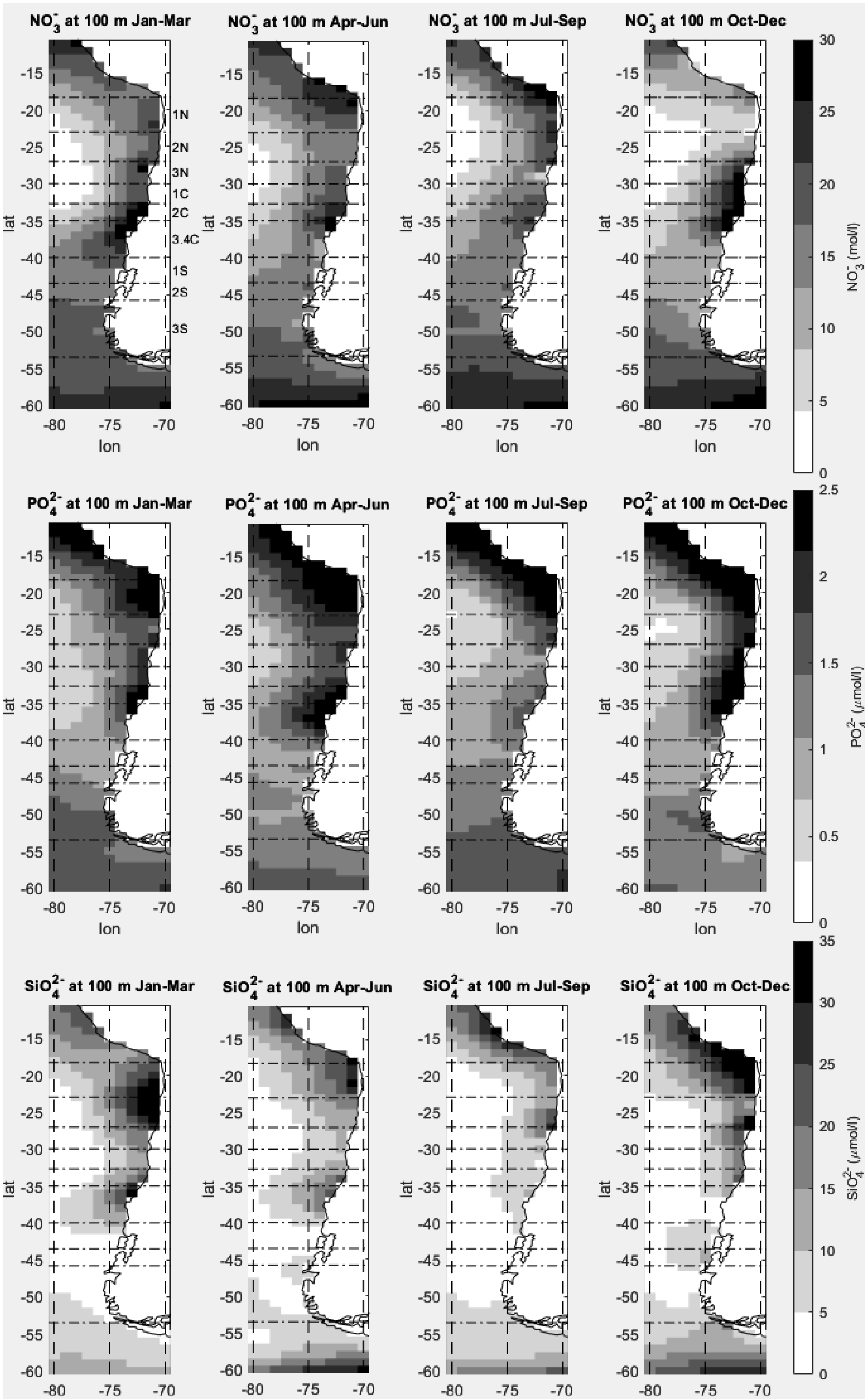

Figure 5. NO_3^- (mol·L^{-1}), PO_4^{2-} (µmol·L^{-1}), and SiO_4^{2-} (µmol·L^{-1}) seasonal concentrations at 100 m of depth data from García et al. (2010).

4.1.2. Upwelling Nutrient Estimation

For the upwelling WS and ZET were computed using Eqs. 1 and 2 (Table 6). As the idea is to establish which variable is more relevant rather than accurate calculations, EP was not considered.

Table 6. Seasonal average meridional WS ($kg{\cdot}m^{-1}{\cdot}s^{-2}$) and ZET ($m^2{\cdot}s^{-1}$) for the study period (2002-2018). Positive values indicate upwelling while negative downwelling.

Zones	Northern Zone			Central Zone				Southern Zone		
WS	**1NT**	**2NT**	**3NT**	**1CT**	**2CT**	**3CT**	**4CT**	**1ST**	**2ST**	**3ST**
Summer	0.03	0.03	0.05	0.07	0.07	0.09	0.06	0.01	0.01	-0.02
Autumn	0.03	0.04	0.06	0.06	0.03	0.02	0.00	0.00	0.00	-0.01
Winter	0.02	0.05	0.08	0.07	0.03	0.02	0.00	0.00	-0.01	-0.01
Spring	0.02	0.04	0.08	0.10	0.08	0.08	0.04	0.01	0.00	-0.02
ZET	**1NT**	**2NT**	**3NT**	**1CT**	**2CT**	**3CT**	**4CT**	**1ST**	**2ST**	**3ST**
Summer	0.49	0.51	0.72	0.89	0.80	1.03	0.68	0.15	0.07	-0.16
Autumn	0.49	0.66	0.82	0.78	0.37	0.25	0.05	-0.02	-0.04	-0.09
Winter	0.47	0.83	1.13	0.96	0.35	0.20	0.02	-0.03	-0.07	-0.12
Spring	0.46	0.60	1.10	1.32	0.94	0.90	0.38	0.06	0.01	-0.15

The subsections with highest upwelling in the warm season are 3NT, 1CT and 3CT. As expected, the Southern Zone showed a downwelling tendency in the cold season, with 3ST showing downwelling the entire year.

The ZET allows determination of the nutrient brought up by upwelling in each subsection. The Average ZET was multiplied by average subsectional coastal length and then by the average concentration of each nutrient at 100 m depth (Table 7).

Table 7. The average annual nutrient mass flux per subsection brought by the upwelling.

Subsection	ZET m^2/s	Coast length m	NO_3^- 100m kg/m^3	PO_4^{2-} 100m kg/m^3	SiO_4^{2-} 100m kg/m^3	NO_3^- flux T/yr	PO_4^{2-} flux T/yr	SiO_4^{2-} flux T/yr
1NT	0.47	5.50E+05	1023	2.60E-04	2.50E-03	8.40E+12	2.10E+06	2.00E+07
2NT	0.65	4.90E+05	845	1.60E-04	2.00E-03	8.50E+12	1.60E+06	2.00E+07
3NT	0.94	3.80E+05	1279	1.70E-04	1.60E-03	1.40E+13	1.90E+06	1.80E+07
1CT	*0.99*	3.50E+05	1256	1.70E-04	1.20E-03	1.40E+13	1.90E+06	1.30E+07
2CT	0.61	3.10E+05	1550	2.40E-04	1.60E-03	9.20E+12	1.40E+06	9.30E+06
3CT	0.60	1.90E+05	1651	2.50E-04	1.60E-03	6.00E+12	9.00E+05	5.70E+06
4CT	0.28	5.10E+05	891	1.50E-04	1.10E-03	4.10E+12	6.90E+05	4.80E+06
1ST	0.04	5.20E+05	984	1.10E-04	4.60E-04	6.40E+11	7.00E+04	3.00E+05
2ST	-0.005	3.60E+05	-	-	-	-	-	-
3ST	-0.13	1.30E+06	-	-	-	-	-	-

The upwelling was more significant from 3NT to 2CT. Even though 1ST has a low upwelling, this is enough to bring considerable nutrients to the surface. The other two southern subsections have a downwelling tendency, so their ZETs were not estimated.

4.1.3. Precipitation Nutrient Estimation

The PR concentrations obtained by Baker et al. (2010) were multiplied by the average annual PR (2002-2018) per subsection and by the ocean area considering 100 km of width to obtain the nutrient mass (Table 8). These results show that precipitation adds a small quantity of nutrients. The sections with higher inputs are from 4CT to 3ST.

TABLE 8. THE AVERAGE ANNUAL NUTRIENT MASS FLUX PER SUBSECTION CONTRIBUTED BY THE PR.

Subsection	PR m/yr	Coast length m	PR m^3/yr	NO_3^- flux T/yr	PO_4^{2-} flux T/yr
1NT	0.03	5.50E+05	1.60E+09	2.80E-04	1.90E-06
2NT	0.03	4.90E+05	1.70E+09	3.00E-04	2.00E-06
3NT	0.04	3.80E+05	1.60E+09	2.80E-04	1.90E-06
1CT	*0.14*	3.50E+05	4.80E+09	8.30E-04	5.60E-06
2CT	0.40	3.10E+05	1.20E+10	2.10E-03	1.40E-05
3CT	0.68	1.90E+05	1.30E+10	2.60E-03	1.70E-05
4CT	1.05	5.10E+05	5.40E+10	1.20E-02	7.40E-05
1ST	1.30	5.20E+05	6.80E+10	1.50E-02	9.40E-05
2ST	1.490	3.60E+05	5.40E+10	1.20E-02	7.50E-05
3ST	1.01	1.30E+06	1.30E+11	2.90E-02	1.90E-04

4.1.4. Main River Nutrient Estimation

The Northern Zone does not have many rivers due to its intense aridity (Thiel et al., 2007). The Central Zone has many well-spaced rivers that add nutrients to the mixed layer (Masotti et al., 2018; Thiel et al., 2007). Examples of these are Maipo (33.72°S), Mataquito (34.98°S) and Maule Rivers (35.41°S), but the most relevant are the Itata (36.47°S) and Biobio Rivers (36.84°S; Vergara et al., 2017; Masotti et al., 2018). Massotti et al. (2018) reported that these add 0.16-169 and 0.05-$10.3{\cdot}10^6$ nmol m^{-3} NO_3^- and PO_4^{2-}.

The nutrient discharge for the main rivers in the Central Zone was studied by Masotti et al. (2018), showing that the highest flux occurs during the winter and the river with the highest nutrient contribution is Biobio (Table 9). The nutrients discharged by the main Southern Zone rivers (Table 10) were computed based on the averaged fluxes during the study period (CR2,2018). Then, they were multiplied by the typical nutrient concentrations reported by Castro (2010). Tables 9 and 10 show the nutrient addition per subsection. As SiO_4^{-2} was not computed by Masotti et al. (2018), it was not calculated for the southern rivers either.

TABLE 9. AVERAGE ANNUAL NUTRIENTS ADDED BY THE MAIN RIVERS IN THE CENTRAL ZONE COMPELLED PER SUBSECTION. COLUMNS 3-6 ARE FROM (MASOTTI ET AL., 2018).

Subsection	Rivers	NO_3^- winter T/mnth	NO_3^- rest T/mnth	PO_4^{2-} winter T/mnth	PO_4^{2-} rest T/mnth	Total NO_3^- flux T/yr	Total PO_4^{2-} flux T/yr
2CT	Maipo	160	80	12	4	**1.29E+03**	**9.3E+01**
	Mataquito	16	5	4	1		
3CT	Maule	40	16	12	4	**2.64E+02**	**7.2E+01**
4CT	Itata	120	10	6	2	**2.63E+03**	**3.5E+02**
	Biobio	245	160	45	20		

The Southern Zone has many rivers with high fluxes. The most relevant are Puelo (41.60°S), Yelcho (42.98°S), Palena (43.82°S), Cisnes (44.75°S), Aysén (45.41°S), Baker (47.02°S) and Pascua (48.23°S; CR2,2018). The Southern rivers bring low NO_3^- and PO_4^{2-} concentrations on average to the ocean (1.5 and $0.11{\cdot}10^7$ nmol m^{-3}) with low variations per season, while SiO_4^{2-} varies from 4 to 15 10^5 nmol m^{-3} (Castro, 2010; De La Torre, 2016).

Table 10. Average annual nutrients added by the main rivers in the Southern Zone compelled per subsection.

Subsection	Rivers	Flux m^3/s	Flux m^3/yr	NO_3^- T/yr	PO_4^{2-} T/yr	Total NO_3^- T/yr	Total PO_4^{2-} T/yr
1ST	**Puelo**	615	1.90E+10	1804	203	**3.13E+03**	**3.5E+02**
	Yelcho	452	1.40E+10	1326	149		
2ST	**Palena**	782	2.50E+10	2293	258	**4.45E+03**	**5E+02**
	Cisnes	214	6.80E+09	628	71		
	Aysén	522	1.70E+10	1531	172		
3ST	**Baker**	870	2.70E+10	2552	287	**4.24E+03**	**4.8E+02**
	Pascua	574	1.80E+10	1683	189		

Tables 9 and 10 show that rivers add in thousands of tonnes per year, while precipitation (Table 8) adds a nutrient flux around kilograms per year. The nutrient flux added by rivers was slightly higher in the Southern Zone. However, this mass is not as significant compared with the nutrient brought by upwelling (Table 7).

4.2. Analysis per Zone

The phytoplankton highest concentrations were detected in 3CT-1ST (Figure 3 and Table 4). In contrast, the Upwelling analysis (Table 7) showed that nutrient addition is relatively similar from 1NT to 4CT with slightly higher values in 3NT and 1CT, while in the Southern Zone it was negative. This means that other factors must be considered such as the shelf width. The climatic indices contribution is not explicitly covered here but will be the subject of a later paper.

4.2.1. Northern Zone

The results revealed that the Northern Zone had a low phytoplankton concentration with small seasonal variability, except in 1NT. This pattern is due to weak winds (1NT-2NT), and a lack of precipitation (Tables 4 and 5). However, the upwelling was significant (Table 7). As a result of these stable weather conditions driven by the SPSA this Zone is a High Nutrient Low Chlorophyll (HNLC) region (Yuras et al., 2005; Ancapichun and Garcés, 2015; Thiel et al., 2007).

1NT presented a higher Chl concentration but this was almost constant, with a slight rise in September and February. These results are consistent with the background surface nutrient maps that showed a higher nutrient concentration in this Zone (Figure 4). This Chl activity and high nutrient level are likely related to the increased production from neighbouring Peruvian waters, which has a constant Ekman transport that allows a constant nutrient supply (Thiel et al., 2007; Echevin et al., 2014). Furthermore, these nutrients are transported through Chile by poleward Equatorial Subsurface Water (ESSW) from northern Peru (Thiel et al., 2007; Echevin et al., 2014). Also, this subsection has a broad shelf in comparison to the rest of the Northern Zone which in places is less than 10 km (Ancapichun and Garcés, 2015; Thiel et al., 2007; Cortés et al., 2017).

Even though 2NT has filaments in Mejillones and Antofagasta associated with capes, these were not productive, likely related to their narrow shelf and anthropic activities there; effectively these were more productive during the nineties (Thiel et al., 2007; Camus and Hajek, 1998). The Chl in 3NT showed a weak seasonal cycle with a maximum value in September that seems to be partly triggered by its high VW, having a more statistically significant correlation (P-value <0.01, Rho=0.21; Table 5). This subsection should have a significant upwelling, but the narrow shelf seems to affect this region as well (Table 7).

Overall, the constant but low southerly winds and scarce precipitation in this Zone, driven by the SPSA, lead to a low nutrient renovation process in the euphotic layer, which is even more limited by a shelf less than 10 km wide, not allowing a full remineralisation process (Thiel et al., 2007; Marchant et al., 2007). The only exception is in 1NT, which has nutrients from Peru and a slightly broader shelf within the Peruvian limits.

4.2.2. Central Zone

The Central Zone presented a seasonally varying production, with a high Chl concentration during the summer and spring (Corredor-Acosta et al., 2015; Gómez et al., 2017). This is linked to the SPSA movement and the sunlight reduction during the winter. The SPSA in the warm season leads to production of a strong eddy that enhances the upwelling from 30°S to 38°S (Thiel et al., 2007). The seasonal difference was more pronounced in 3CT-4CT, leading to higher PR with more well-spaced rivers and lower southerly winds with a westerly component during the winter, while 1CT-2CT exhibited more significant longshore winds the entire year (Tables 3 and 4). However, the southerly winds have similar values in the whole Central Zone during the summer. Therefore, Chl~VW were statistically significant in the whole Zone, excluding 2CT. Indeed, the Chl~VW were higher in 3CT-4CT (0.27, 0.38; Table 5) but also Chl~UW (0.2, -0.27).

These results demonstrate that 3CT-4CT had a high production compared with 1CT-2CT, despite the last having a more significant ZET driven by the southerly winds (Table 7). One plausible reason for this is that 3CT-4CT has a higher PR and more rivers, but section 3.2 showed that these factors do not increase the nutrient addition as much as the upwelling. However, another factor influencing the differences in these two groups is the shelf configuration, which is less than 10 km wide in 1CT and 2CT, while the average width for 3CT and 4CT is 40 to 70 km, except for the middle section in 4CT, where the shelf is 12 km wide. Also, 4CT has a marked Chl filament due to its cape (Thiel et al., 2007; Marchant et al., 2007).

Therefore, this Zone can be split into two: 1CT-2CT with higher winds but narrow shelf, leading to a low Chl concentration and 3CT-4CT, with a marked season with slightly low winds but a more broad shelf leading to a high Chl concentration. Thus, the differences in the Chl signal in these two groups are evidently related to the width of their shelves.

4.2.3. Southern Zone

Although the Southern Zone has a downwelling tendency (Table 7), 1ST and 2ST Chl concentrations showed a seasonal cycle with a high production analogous to 4CT and 3CT, respectively. However, their production was lower during the winter. Meanwhile, 3ST's Chl was almost constant throughout the year but with a moderate Chl concentration, despite the relatively constant northerly winds and few occasions of southerly winds in the winter, with significant westerly winds that were more intense in the winter.

These weather conditions occur because this Zone is at the limits of the SPSA effect. Thus, weak longshore winds are often seen in 1ST during the warm season (Table 3), whereas they occasionally appear in 2ST during the summer. Instead, storms with prominent westerly winds coming from the South Pacific frequently arrived, driven by negative AAO (González-Reyes and Muñoz, 2013; Aguayo et al., 2021). In any case, both wind components strongly impacted the Chl concentration in 1ST (VW=0.45, UW=-0.41; Table 5), while UW had a bigger influence on 3ST's Chl (VW=0.23, UW=-0.32), and 2ST's Chl was affected by both but in a minor way (VW=0.26, UW=-0.29).

Although the nutrient addition by rivers and precipitation is higher in the Southern Zone (Table 10), with a higher flux during the warm season, studies have mentioned that they generate more stratification reducing the phytoplankton response (Landaeta et al., 2011; Aracena et al., 2011; De La Torre, 2016). Thus, Chl~PR (Table 5) in this Zone showed a significant negative relationship, especially in 1ST (-0.39), while 2ST and 3ST were slightly lower (-0.24, -0.2). This is even more evident considering that the background surface nutrients are significant (Figure 4). Effectively authors like Aguayo et al. (2021) have reported that the big drought of (2010-2018) and the positive tendency of AAO in later years reduced the precipitation and river fluxes in the south with a generally positive effect on phytoplankton.

Therefore, the Chl is significant in this region as a result of its high surface nutrient content, and not necessarily just from upwelling. Effectively, the 1ST-2ST high Chl seasonal behaviour likely occurs due to a low PR and river flux during the warm season. Moreover, this effect is even more boosted by a wider shelf width of over 70 km (Strub et al., 2019; Marchant et al., 2007; Aracena et al., 2011).

5. Conclusion

Although 1ST and 2ST typically exhibited westerly winds and excessive precipitation that reduced the phytoplankton proliferation, these are significantly reduced when the SPSA is pushed southwards during the summer leading to higher longshore winds and lower westerly winds and Precipitation events. Recent events such as the big drought of (2010-2018) and the more positive AAO tendency have exacerbated this situation.

Although the upwelling analysis showed that the upwelling has a significant role in nutrient addition in the Northern Zone, the southerly wind and ocean temperatures did not show a significant correlation with the Chl. This is possibly related to the narrow shelf here.

On the other hand, 1NT and 3ST also have a significant Chl activity associated with a broad shelf and the sub-surface currents adding nutrients on the surface. This is supported by the significant nutrient concentration in the Peruvian Zone (Figure 4). In any case, it can be inferred that the Southern Zone has a high nutrient concentration that does not require upwelling, especially 3ST.

Overall, this study has demonstrated the importance of shelf width and the effect the upwelling driven by the presence or absence of the SPSA in the Chilean coast fertilisation, increasing the phytoplankton. Thus, the most productive region is from 3CT to 1ST, owing to both variables being present.

Acknowledgements

F. Tornquist thanks to the Chilean National Agency for Research and Development (ANID) for its financial support. We also want to thank GIOVANNI where this data was extracted, Dr Ricardo Torres and Dr Julie M Jones for their comments and feedback about this material.

CReDiT roles

F. Tornquist: Methodology, Investigation, Writing and Original draft.

G. R. Bigg: Supervision, Conceptualisation, Reviewing and Editing.

R. G. Bryant: Supervision, Conceptualisation and Reviewing.

References

Abbas, M.M., Melesse, A.M., Scinto, L.J. and Rehage, J.S. (2019). Satellite estimation of chlorophyll-a using moderate resolution imaging spectroradiometer (MODIS) sensor in shallow coastal water bodies: Validation and improvement. Water, 11(8), p.1621.

Aguayo, R., León-Muñoz, J., Garreaud, R., & Montecinos, A. (2021). Hydrological droughts in the southern Andes (40–45°S) from an ensemble experiment using CMIP5 and CMIP6 models. Sci Rep, 11(1), 5530-5516. https://doi.org/10.1038/s41598-021-84807-4

Aguirre, C., Flores-Aqueveque, V., Vilches, P., Vásquez, A., Rutllant, J. A., & Garreaud, R. (2021). Recent changes in the low-level jet along the subtropical west coast of South America. Atmosphere, 12(4), 465. https://doi.org/10.3390/atmos12040465

Ancapichun, S., & Garcés-Vargas, J. (2015). Variability of the Southeast Pacific Subtropical Anticyclone and its impact on sea surface temperature off north-central Chile. Ciencias marinas, 41(1), 1-20. https://doi.org/10.7773/cm.v41i1.2338

Aracena, C., Lange, C. B., Iriarte, J.L., Rebolledo, L., & Pantoja, S. (2011). Latitudinal patterns of export production recorded in surface sediments of the Chilean Patagonian fjords (41–55°S) as a response to water column productivity. *Continental shelf research*, *31*(3), 340-355. https://doi.org/10.1016/j.csr.2010.08.008

Baker, A. R., Lesworth, T., Adams, C., Jickells, T. D., & Ganzeveld, L. (2010). Estimation of atmospheric nutrient inputs to the Atlantic Ocean from 50°N to 50°S based on large-scale field sampling: Fixed nitrogen and dry deposition of phosphorus. *Global Biogeochem. Cycles*, *24*(3), n/a. https://doi.org/10.1029/2009GB003634.

Barrett, B. S., Garreaud, R. D., & Falvey, M. (2009). Effect of the Andes Cordillera on precipitation from a midlatitude cold front. Monthly weather review, 137(9), 3092-3109. https://doi.org/10.1175/2009MWR2881.1

Bravo, L., Ramos, M., Astudillo, O., Dewitte, B., & Goubanova, K. (2016). Seasonal variability of the Ekman transport and pumping in the upwelling system off central-northern Chile (~30°S) based on a high-resolution atmospheric regional model (WRF). *Ocean science*, *12*(5), 1049-1065. https://doi.org/10.5194/os-12-1049-2016

Camus P, & Hajek E. (1998). Historia Ambiental de Chile (first ed.). Vol 1. 226 pp https://www.ecolyma.cl/documentos/hist_amb_chile_v1.pdf

Castro, J. (2010). Estimación del balance biogeoquímico del nitrógeno y fósforo inorgánico disuelto en el estero Reloncaví en invierno y primavera de 2004, 2005 y 2006. Universidad Católica de Valparaíso.

CONAMA. (2008). Biodiversidad de Chile, Patrimonio y Desafíos (second ed.), Tomo I.

https://www.academia.edu/28661207/BIODIVERSIDAD_DE_CHILE_PATRIMONIO_Y_DESAFÍOS_TRADICIONES_CULTURALES_Y_BIODIVERSIDAD

Cordero, R. R., Asencio, V., Feron, S., Damiani, A., Llanillo, P. J., Sepulveda, E., Jorquera, J., Carrasco, J. & Casassa, G. (2019). Dry-Season Snow Cover Losses in the Andes (18°–40°S) driven by Changes in Large-Scale Climate Modes. Sci Rep, 9(1), 16945-16910. https://doi.org/10.1038/s41598-019-53486-7

Corredor-Acosta, A., Morales, C. E., Hormazabal, S., Andrade, I., & Correa-Ramirez, M. A. (2015). Phytoplankton phenology in the coastal upwelling region off central-southern Chile (35°S–38°S): Time-space variability, coupling to environmental factors, and sources of uncertainty in the estimates. Journal of Geophysical Research: Oceans, 120(2), 813-831. https://doi.org/10.1002/2014JC010330

Cortés, P., Catalán, P. A., Aránguiz, R., & Bellotti, G. (2017). Tsunami and shelf resonance on the northern Chile coast. Journal of geophysical research. Oceans, 122(9), 7364-7379. https://doi.org/10.1002/2017JC012922

CR2. (2018). Flow data of the rivers of Chile. https://www.cr2.cl/datos-de-caudales/

De la Torre, M. (2016). Variabilidad Espacio-Temporal de la Clorofila y Temperatura Satelital en el Mar Interior de Chiloé y su Relación con Procesos Oceanográficos en el Periodo 2003-2014 Universidad de Concepción.

Echevin, V., Albert, A., Lévy, M., Graco, M., Aumont, O., Piétri, A., & Garric, G. (2014). Intraseasonal variability of nearshore productivity in the Northern Humboldt Current System: The role of coastal trapped waves. Continental Shelf Research, 73, 14-30. https://doi.org/10.1016/j.csr.2013.11.015

Falkowski, P. (1994). The role of phytoplankton photosynthesis in global biogeochemical cycles. Official Journal of the International Society of Photosynthesis Research, 39(3), 235-258. https://doi.org/10.1007/BF00014586

Ferreira, A., Sá, C., Silva, N., Beltrán, C., Dias, A.M. and Brito, A.C. (2020). Phytoplankton community dynamics in a coastal bay under upwelling influence (Central Chile). Estuarine, Coastal and Shelf Science, 245, p.106968.

Franz, B. A., Werdell, P. J., Meister, G., Bailey, S. W., Epleejr, R. E., Feldman, G. C., Kwiatkowskaa, E., McClain, C., Patt, F., & Thomas, D. (2005). The continuity of ocean color measurements from SeaWiFS to MODIS. In (Vol. 5882, pp. 58820W-58820W-58813).

García, H. E., R. A. Locarnini, T. P. Boyer, J. I. Antonov, M. M. Zweng, O. K. Baranova, and D. R. Johnson, (2010). World Ocean Atlas 2009, Volume 4: Nutrients (phosphate, nitrate, silicate). S. Levitus, Ed. NOAA Atlas NESDIS 71, U.S. Government Printing Office, Washington, D.C., 398 pp.

García-Reyes, M., Sydeman, W.J., Schoeman, D.S., Rykaczewski, R.R., Black, B.A., Smit, A.J. and Bograd, S.J. (2015). Under pressure: Climate change, upwelling, and eastern boundary upwelling ecosystems. Frontiers in Marine Science, 2, p.109.

Garreaud, R. D. (2009). The Andes climate and weather. Advances in geosciences, 22(22), 3-11. https://doi.org/10.5194/adgeo-22-3-2009

Garreaud, R. D., Boisier, J. P., Rondanelli, R., Montecinos, A., Sepúlveda, H. H., & Veloso-Aguila, D. (2020). The Central Chile Mega Drought (2010–2018): A climate dynamics perspective. International journal of climatology, 40(1), 421-439. https://doi.org/10.1002/joc.6219

Gómez, F., Montecinos, A., Hormazabal, S., Cubillos, L. A., Correa-Ramirez, M., & Chavez, F. P. (2012). Impact of spring upwelling variability off southern-central Chile on common sardine (Strangomera bentincki) recruitment. Fisheries Oceanography, 21(6), 405-414. https://doi.org/10.1111/j.1365-2419.2012.00632.x

Gómez, F. A., Spitz, Y. H., Batchelder, H. P., & Correa-Ramirez, M. A. (2017). Intraseasonal patterns in coastal plankton biomass off central Chile derived from satellite observations and a biochemical model. Journal of Marine Systems, 174(C), 106-118. https://doi.org/10.1016/j.jmarsys.2017.05.003

González-Reyes, Á., & Muñoz, A. A. (2013). Cambios en la precipitación de la ciudad de Valdivia (Chile) durante los últimos 150 años. Precipitation changes of Valdivia city (Chile) during the past 150 years, 34(2), 191-200. https://doi.org/10.4067/S0717-92002013000200008

Iriarte, J.L., González, H.E., Liu, K.K., Rivas, C. and Valenzuela, C. (2007). Spatial and temporal variability of chlorophyll and primary productivity in surface waters of southern Chile (41.5–43 S). Estuarine, Coastal and Shelf Science, 74(3), pp.471-480.

Jacob, B., Daneri, G., Quiñones, R.A. and Sobarzo, M. (2011). Community metabolism, phytoplankton size structure and heterotrophic prokaryote production in a highly productive upwelling zone off northern Chile. Marine Ecology Progress Series, 430, pp.23-34.

Landaeta, M., Bustos, C., Palacios-Fuentes, P., Rojas, P., & Balbontin, F. (2011). Ichthyoplankton distribution in South Patagonia, Chile: potential effects of ice melting from the Southern Ice Field. Latin American journal of aquatic research (LAJAR), 39(2), 236-249. https://doi.org/10.3856/vol39-issue2-fulltext-5

Lara, C., Miranda, M., Montecino, V., & Iriarte, J.L. (2010). Chlorophyll-a MODIS mesoscale variability in the Inner Sea of Chiloé, Patagonia, Chile (41-43 degrees S): Patches and Gradients? Rev. Biol. Mar. Oceanogr., 45(2), 217-225.

Liao, X., Zhan, H., & Du, Y. (2016). Potential new production in two upwelling regions of the western Arabian Sea: Estimation and comparison. *Journal of geophysical research. Oceans*, *121*(7), 4487-4502. https://doi.org/10.1002/2016JC011707

Marchant, M., Cecioni, A., Figueroa, S., González, H., Giglio, S., Hebbeln, D., Kaiser, J., Lamy, F., Mohtadi, M., Pineda, V., & Romero, O. (2007). Marine Geology, Oceanography and climate. In T. Moreno & W. Gibbons (Eds.), The Geology of Chile (first ed., pp. 288-293). The Geological Society.

Masotti, I., Aparicio-Rizzo, P., Yevenes, M. A., Garreaud, R., Belmar, L., & Farías, L. (2018). The influence of river discharge on nutrient export and phytoplankton biomass off the Central Chile Coast (33°-37°S): Seasonal cycle and interannual variability. Frontiers in Marine Science, 5. https://doi.org/10.3389/fmars.2018.00423

Mogollón, R., & Calil, P. H. R. (2017). On the effects of ENSO on ocean biogeochemistry in the Northern Humboldt Current System (NHCS): A modeling study. Journal of Marine Systems, 172, 137-159. https://doi.org/10.1016/j.jmarsys.2017.03.011

NASA. (2018). chlorophyll a. https://oceancolor.gsfc.nasa.gov/atbd/chlor_a/

Schulz, N., Boisier, J. P., & Aceituno, P. (2012). Climate change along the arid coast of northern Chile. Int. J. Climatol, 32(12), 1803-1814. https://doi.org/10.1002/joc.2395

Strub, P. T., James, C., Montecino, V., Rutllant, J. A., & Blanco, J. L. (2019). Ocean circulation along the southern Chile transition region (38°–46°S): Mean, seasonal and interannual variability, with a focus on 2014–2016. *Prog Oceanogr*, *172*, 159-198. https://doi.org/10.1016/j.pocean.2019.01.004

Thiel, M., Macaya, E., Acuna, E., Arntz, W., Bastias, H., Brokordt, K., Camus, P., Carlos Castilla, J., Castro, L., Cortes, M., Dumont, C., Escribano, R., Fernandez, M., Gajardo, J., Gaymer, C., Gómez, I., Gonzalez, A., González, H., Haye, P., & Alonso Vega, J. (2007). The Humboldt Current System of Northern and Central Chile. In Oceanographic Processes, Ecological Interaction and Socioeconomic Feedback (Vol. 45, pp. 195-344). Oceanography and Marine Biology: An Annual Review.

Thompson, P. A., O'Brien, T. D., Paerl, H. W., Peierls, B. L., Harrison, P., & Robb, M. (2015). Precipitation as a driver of phytoplankton ecology in coastal waters: A climatic perspective. Estuarine, Coastal and Shelf Science, 162, 119-129. https://doi.org/10.1016/j.ecss.2015.04.004

Vergara, O. A., Echevín, V., Sepúlveda, H. H., & Quiñones, R. A. (2017). Controlling factors of the seasonal variability of productivity in the southern Humboldt Current System (30–40°S): A biophysical modeling approach. Continental Shelf Research, 148, 89-103. https://doi.org/10.1016/j.csr.2017.08.013

Xiao, C., Ye, J., Esteves, R. M., & Rong, C. (2016). Using Spearman's correlation coefficients for exploratory data analysis on big dataset. Concurrency and Computation: Practice and Experience, 28(14), 3866-3878. https://doi.org/10.1002/cpe.3745

Yang, M. M., Ishizaka, J., Goes, J. I., Gomes, H. d. R., Maúre, E. d. R., Hayashi, M., Katano, T., Fujii, N., Saitoh, K., Mine, T., Yamashita, H., & Mizuno, A. (2018). Improved MODIS-Aqua chlorophyll-a retrievals in the turbid semi-enclosed Ariake Bay, Japan. Remote sensing (Basel, Switzerland), 10(9), 1335. https://doi.org/10.3390/rs10091335

Yuras, G., Ulloa, O., & Hormazábal, S. (2005). On the annual cycle of coastal and open ocean satellite chlorophyll off Chile (18°–40°S. Geophysical Research Letters, 32(23), n/a-n/a. https://doi.org/10.1029/2005GL023946